# Single Cell Nanobiosensors for Dynamic Gene Expression Profiling in Native Tissue Microenvironments

*Shue Wang, Reza Riahi, Na Li, Donna D. Zhang, and Pak Kin Wong**

The tissue microenvironment plays crucial roles in the regulation of various cell functions.[1] Despite the available biosensing techniques, such as microfluidics,[2] RNA in situ hybridization,[3,4] and single cell transcriptomics,[5] dynamic profiling of gene expression in complex tissue structures at the single cell level remains a challenging task. Current approaches for characterizing cell–cell and cell–microenvironment interactions are often limited because they are based on the fixation or physical isolation of cells to identify specific phenotypes. Features of the tissue architectures, such as hierarchical organization of cells and cell-to-cell coordination, as well as dynamic behaviors of cells, are inherently lost when cells are studied in isolation or fixed. Therefore, novel technologies that allow for dynamic monitoring of gene expression in individual cells in native tissue microenvironments will enable new approaches in elucidating unrecognized characteristics and regulatory processes of the cells and develop novel therapeutic approaches.

The advent of nanoengineered and synthetic materials enables new opportunities in developing biosensor platforms for dynamic single cell gene expression analysis.[6–8] Molecular and nanoengineered biosensors, such as molecular beacons,[9,10] nanoflares,[11–13] and displacement probes,[14,15] have been reported for intracellular sensing in living cells. Nevertheless, major challenges exist for single cell gene expression analysis in complex tissue microenvironments.[16–18] For instance, the nanoscale or molecular biosensors should be effectively delivered into viable tissues with minimal toxicity to the cells, particularly for cells that are sensitive to biochemical perturbation. Ideally, the transfection method should allow massively parallel delivery and have an ability to penetrate into the tissues.[19] The method should also be generally applicable to different cell and tissue types. In addition, intracellular sensing requires the biosensors to be inert to nonspecific binding and stable in the cells for the duration of the experiment. The binding dynamics of the biosensor and target molecules should also be elucidated systematically to facilitate the design of the biosensor for optimizing the sensitivity, specificity, and dynamic response.

To address the unmet needs, we present a biosensor using nanoparticles and fluorophore-labeled locked nucleic acid probes (LNA) for monitoring spatiotemporal gene expression dynamics in complex cell structures and native tissue microenvironments at the single cell level. In this study, two nanoparticles, namely, a spherical gold nanoparticle (GNP) and a gold nanorod (GNR), with different sizes, coating and shapes are evaluated to monitor single cell gene expression dynamics in living cells and tissues. We focus our study on the ability of the biosensor for dynamic single cell gene expression profiling in native tissue microenvironments. An equilibrium analysis along with experimental measurement is performed to elucidate the characteristics of the nanoparticle-LNA interactions and optimize the sensing performance of the biosensor. The biosensor is optimized for monitoring spatiotemporal mRNA expression in primary human cells, capillary networks in vitro, and various animal tissues, including skin, retina and cornea tissues. Mechanically injured cornea tissues are also studied to demonstrate the ability of the biosensor for monitoring single cell gene expression dynamics in native tissue microenvironments.

The biosensor consists of gold nanoparticles and LNA probes (**Figure 1**a). The LNA probe is a 20-base nucleic acid sequence labeled with a fluorophore (6-FAM) at the 5′ end. Alternating LNA/DNA oligonucleotides are utilized to optimize the sensitivity, specificity and intracellular stability.[20,21] LNA is a modified RNA nucleotide in which the 2′ oxygen and 4′ carbon of the ribose are joined through a methylene bridge. The bridge "locks" the structure into a rigid conformation. Compared to traditional DNA and RNA, the LNA oligonucleotide has higher melting temperature and binding selectivity. These properties of LNA lead to outstanding sensitivity and specificity for hybridization. The LNA also enhances the stability of the probe, which enables intracellular gene expression monitoring in complex tissue microenvironment. The LNA binds spontaneously to the nanoparticle to form nanoparticle-LNA complexes due to the affinity between the LNA and gold nanoparticles. In the complexes, the close proximity between the fluorophore and gold nanoparticle facilitates effective energy transfer to quench the excited state of the fluorophore.[22] In the presence of the target

S. Wang, Prof. P. K. Wong
Department of Aerospace and Mechanical Engineering
The University of Arizona
Tucson, AZ 85721, USA
E-mail: pak@email.arizona.edu
R. Riahi
Harvard-MIT Health Sciences and Technology
Massachusetts Institute of Technology and Harvard Medical School
Cambridge, MA 02139, USA
Prof. N. Li
Department of Mechanical and Aerospace Engineering
University of Miami
Coral Gables, FL 33146, USA
Prof. D. D. Zhang
Department of Pharmacology and Toxicology
University of Arizona
Tucson, AZ 85724, USA
Prof. P. K. Wong
Department of Biomedical Engineering and Department of Mechanical and Nuclear Engineering
The Pennsylvania State University
University Park, PA 16802, USA

**DOI: 10.1002/adma.201502814**

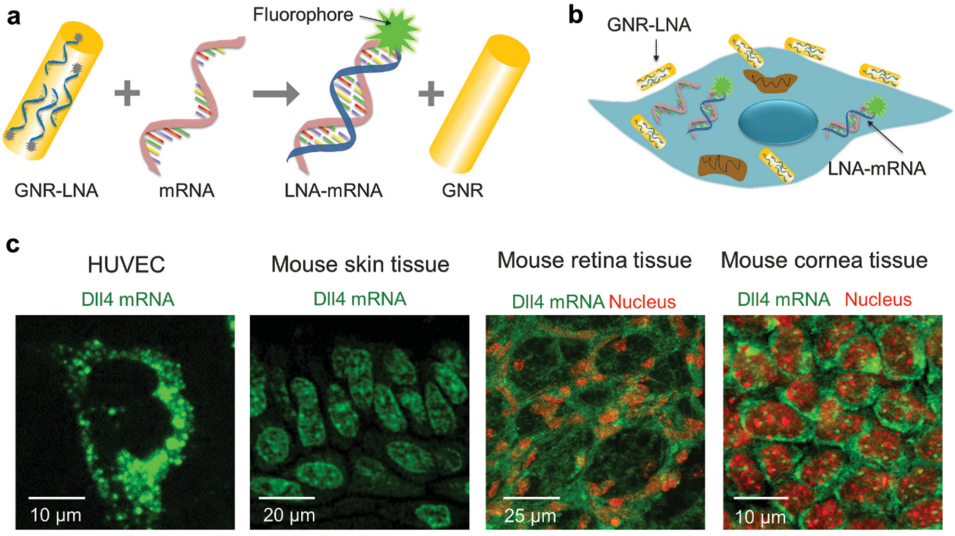


**Figure 1.** GNR-LNA for single cell gene expression analysis in living cells and tissues. a) Schematic of the GNR-LNA biosensor. b) Endocytic uptake of the GNR-LNA probe by cells for intracellular detection. c) Dll4 mRNA gene expression (green) in HUVEC, mouse skin, retina, and cornea tissues. For mice retina and cornea tissues, the nuclei of epithelial cells were stained using TO-PRO-3, cytoplasm of epithelium cells were recognized by Dll4 probe. Images are representative of three independent experiments.

mRNA, the LNA probe is thermodynamically displaced from the gold nanoparticle and binds to the specific mRNA target sequence due to the higher binding affinity. The binding reaction physically displaces the LNA probe from the nanoparticle, allowing the fluorophore to emit light. The competitive binding process is dynamic and reversible. The concentration of the target mRNA can, therefore, be measured dynamically based on the fluorescence intensity in each individual cell.

The nanoparticle-LNA probes can be internalized by cells for detecting mRNA in the cytoplasm (Figure 1b), providing an effective approach for probing the spatiotemporal gene expression dynamics in native tissue microenvironments. In particular, the nanoparticle-LNA complexes are internalized via endocytosis when incubating with living cells.[23] The procedure, which does not require transfection or physical injection, allows massively parallel delivery and minimizes perturbation to the cells. The noninvasiveness of the procedure is particularly important for studying primary cells and viable tissues that are sensitive to biochemical and physical manipulation. We characterized the experimental procedure, including the incubation concentration and time, to control cellular uptake of GNR-LNA and GNP-LNA complexes (Figure S1, Supporting Information). At low concentrations of the nanoparticle-LNA complexes (e.g., below 24 μg $mL^{-1}$), the cells displayed normal morphology and the viability is comparable to untreated cells (Figure S2, Supporting Information). The biosensor is compatible with primary human cells and various tissue types. Figure 1c shows the detection of delta-like ligand 4 (Dll4) expressions in human umbilical vein endothelial cells (HUVEC), mouse skin, mouse retina, and mouse cornea at the single cell level.

The characteristics and sensing performance of GNR and GNP were studied. The spherical GNP was 10 nm diameter and the GNR was 10 nm in diameter and 67 nm in length. The UV–vis-NIR absorption spectra of the GNP and GNR were characterized (Figure S3, Supporting Information). The sensing performances of the GNR-LNA and GNP-LNA probes were evaluated and compared in HUVECs (Figure S4, Supporting Information). Dll4 mRNA expression in individual HUVECs was detectable with both GNR-LNA and GNP-LNA probes. LNA probes targeting $\beta$-actin and random sequences were also tested as positive and negative controls. The biosensors captured the relative abundance of the gene expression, supporting the applicability of the technique (**Figure 2**a). Compared to the GNP-LNA probe, the GNR-LNA probe had a higher signal-to-noise ratio. The maximum signal-to-noise ratios for GNR-LNA probe and GNP-LNA probe were 12.0 and 6.3, respectively. The difference in the signal-to-noise ratios between the GNR and GNP can be understood by the intracellular uptake, surface to volume ratio and binding affinity (Section B, Supporting Information). Overall, the GNR displayed better performance than the GNP and was used to detect intracellular mRNA expression for the rest of the study.

To demonstrate the probes for gene expression analysis in the morphogenesis of cellular structures, the regulation of Dll4 in the formation of in vitro capillary networks was studied.[24–26] The capillary networks were self-assembled by seeding HUVEC on Matrigel.[27] The morphology, viability, and network architecture were similar with and without the probe, suggesting that the GNR-LNA probe did not interfere with the normal functions of the cells. The cells were treated with DAPT (a $\gamma$-secretase inhibitor that blocks Notch signaling) and Jagged1 (a ligand of the Notch pathway), which modulate the Notch-Dll4 signaling pathway (Figure 2b–d).[26] Without treatment, a wide distribution of Dll4 expression was observed in the networks. In particular, a subset of cells expressed a high level of Dll4 in the capillary networks. With DAPT, which blocks Notch intracellular cleavage and signaling, the density of the capillary network was increased. Consistent with the inhibitory role of Notch,[28] DAPT treatment increased the expression of Dll4 mRNA and resulted in a relatively uniform distribution.[29] In

ADVANCED MATERIALS
www.advmat.de

www.MaterialsViews.com

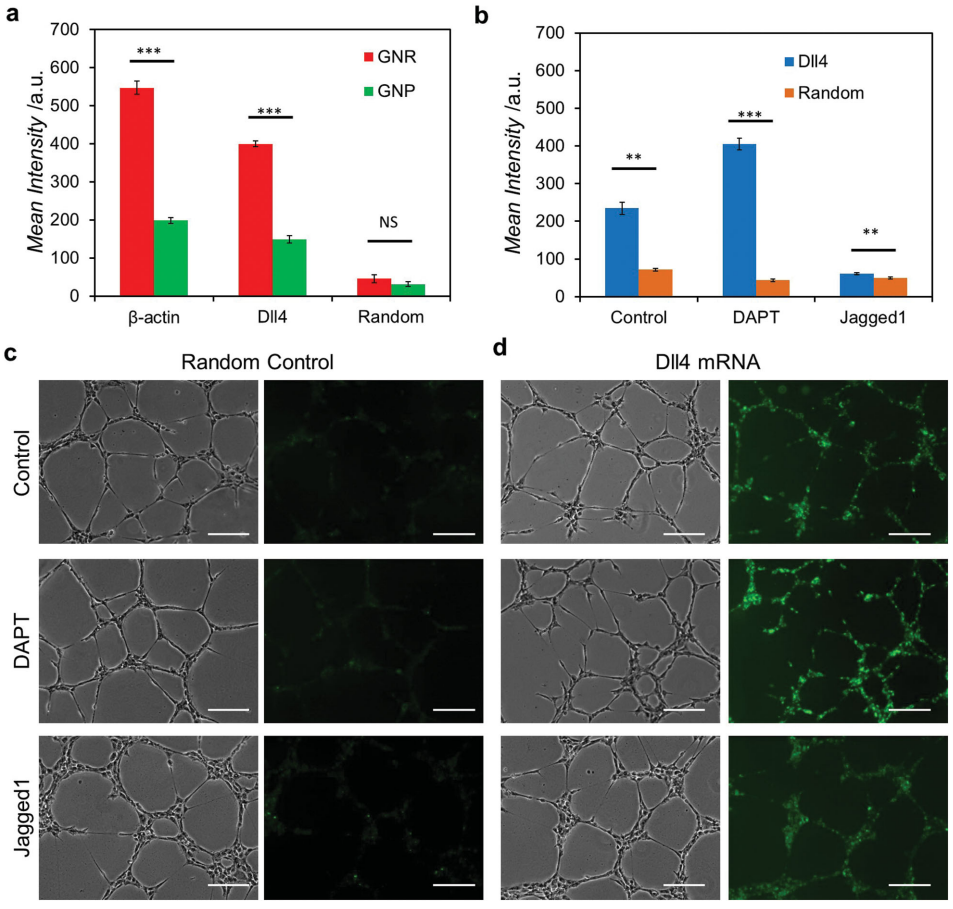


**Figure 2.** Characteristics of nanoparticle-LNA probes for single cell gene expression measurement. a) Mean fluorescence intensities of β-actin, Dll4, and random probes in HUVEC. b) Mean fluorescence intensities of random and Dll4 probes under different treatments. c,d) Bright-field and fluorescence images of HUVEC networks treated with DAPT and Jagged1. Images are representative of at least two independent experiments. Scale bars, 200 μm.

contrast, Jagged1 treatment, which mediates Notch signaling, reduced the Dll4 expression and the density of the capillary networks.

To demonstrate the applicability of the GNR-LNA biosensor for investigating single cell gene expression analysis in intact tissues, the mechanoregulation of Dll4 in mouse cornea tissues was studied. Mechanical force and Dll4 signaling are recently shown to play essential roles in the formation of leader cells during wound healing.[30] Mechanical injury of the cornea tissues was applied to disrupt the cell-cell interactions of corneal epithelial cells and to study the regulation of corneal wound healing.[31] A ROCK inhibitor Y-27632, which reduces the cell traction force,[32] was also injected into mice to perturb the cell traction force pharmacologically. **Figure 3**a,b shows the effects of mechanical injury on Dll4 expression in cornea tissues with and without Y-27632 treatment. The Dll4 expression was estimated by measuring the fluorescence intensity of individual cells in the corneal epithelium (Figure 3e). Both mechanical injury of the cornea and Y-27632 treatment to mice were able to upregulate Dll4 expression. Mechanical injury in the cornea of Y-27632 treated mice enhanced the Dll4 expression synergistically. Furthermore, the expression of Dll4 of single cells near and far away from the mechanical wound were tracked to study the dynamics of injury-induced Dll4 expression. Figure 3c,d shows time-lapse fluorescence images of mouse cornea tissues with and without mechanical injury. The Dll4 expression of six representative cells for each case were traced and analyzed (Figure 3f,g). The Dll4 expression in cells far away from the wound remained constant. The Dll4 expression in cells near the wound was significantly increased. Interestingly, the dynamics of Dll4 expression are highly diverse among different cells, highlighting the inhomogeneity in the injury response. Collectively, these results demonstrate the applicability of the GNR-LNA biosensor for single cell gene expression analysis in native tissues microenvironments.

In summary, this study demonstrates the nanoparticle-LNA biosensor for spatiotemporal mapping mRNA gene expression in living cells and tissues. The GNR-LNA probes were shown to have several inherent advantages. First, mRNA expression can be detected in complex cell structures at the single cell level, which is critical for elucidating the emergency and heterogeneity in complex biological processes. Second, the probe has excellent stability and low toxicity in living cells for dynamic gene expression analysis over 24 h. Third, the technique can be implemented by an incubation step without transfection and injection, which minimizes the perturbation of cells. Furthermore,

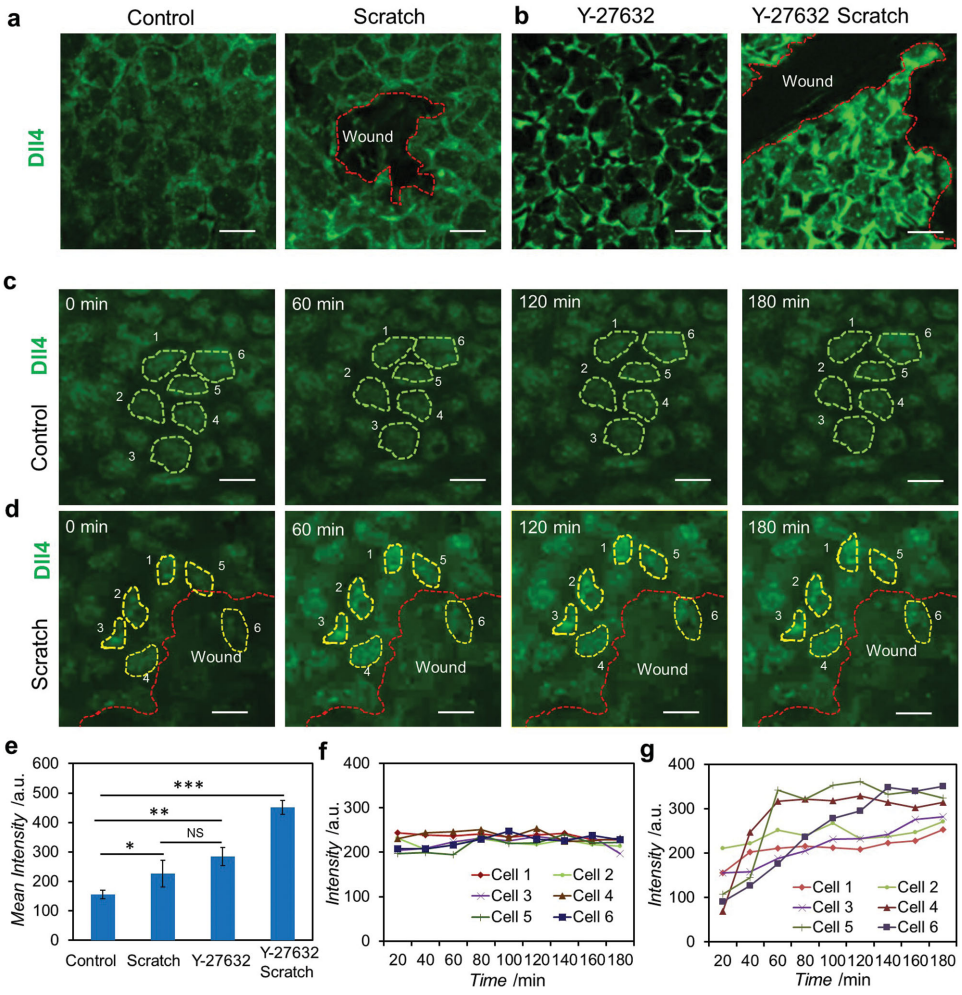


**Figure 3.** Mechanoregulation of Dll4 expression in cornea tissues. a) Dll4 expression in mouse cornea tissue with and without mechanical injury. b) Dll4 expression in mouse cornea tissues with and without mechanical injury from Y-27632 treated mice. c) Time-lapse fluorescence images of a mouse cornea tissue without injury. d) Time-lapse fluorescence images of a mouse cornea tissue after mechanical injury. Scale bars, 20 μm. e) Mean fluorescence intensity of Dll4 expression in mouse cornea tissues, cornea tissues with mechanical injury, Y-27632 treated cornea tissues, and Y-27632 treated cornea tissues with mechanical injury. f) Dynamic Dll4 expression of representative cells without injury. g) Dynamic Dll4 expression in cells near the wound after mechanical injury. Scale bars, 25 μm ($n = 3$).

the technique can be easily adapted to detect different genes and is applicable in various types of cells and tissues, including primary cells and intact animal tissues. These unique characteristics of the GNR-LNA biosensor render the technique a promising approach for dynamic single cell gene expression analysis in tissue morphogenesis and regeneration.[32]

## Experimental Section

*Cell Culture*: Primary human umbilical vein endothelial cells (HUVECs) were obtained from Invitrogen. The cells were cultured in EBM-2 endothelial basal medium with the supplement of 10% fetal bovine serum. Cells were cultured in a humidified incubator at 37 °C and 5% $CO_2$. The media were changed every 2 d. Cells were passaged using trypsin (0.25%) and passage 2–7 was used in the experiments.

*Mice Tissues*: The University of Arizona Institutional Animal Care and Use Committee approved all animal protocols. C57BL/6J mice were fed on laboratory food and tap water ad libitum in a regular 12 h dark/light cycle. The mice were humanely sacrificed at day 7. The eyelids were first cut. Then, the eyes were enucleated using a pair of curved forceps to pinch the optic nerve and ocular muscles. The eyes were transferred to a petri dish containing artificial cerebrospinal fluid solution and placed under a dissecting microscope. All of the fat around the eye was removed. The cornea and iris were cut carefully from the eye. The iris was then removed using a forceps. Then, the lens and sclera were removed without tearing the retina. The cornea and retina were carefully cut into four sectors. The samples were transferred to petri dishes containing 1× DPBS to rinse the tissues. Meantime, the back skin tissues were harvested and cut into 500 μm slices with a Brendel/Vitron Tissue Slicer (VITRON. Inc.). All the harvested tissues were cultured in MEM with 0.5% gentamicin, at 37 °C, 5% $CO_2$, and 100% air humidity incubator.

*Y-27632 Treatment*: Y-27632 (1 μg $g^{-1}$, per mouse) (Sigma-Aldrich, dissolved in DPBS) was injected into mouse once per day at P3, P4, P5, and P6. The mice were sacrificed in a humane way at day 7.

*Single Cell mRNA Gene Detection in Mice Tissues*: The GNR-LNA probes were incubated with the harvested mice retina and cornea at 37 °C, 5% $CO_2$, and with 100% humidity. After 2 h, mice retina tissue and cornea tissue were washed using 1× PBS for three times to remove

extra GNR-LNA probes that are not internalized. The samples were cultured in fresh MEM for imaging.

*Imaging and Statistical Analysis*: Images of HUVECs were captured using an inverted fluorescence microscope with an HQ2 CCD camera. Fluorescence images were taken with the same the exposure time (1 s) and settings for comparison. Images of the animal tissues were captured using Zeiss LSM 510 Meta Confocal Microscope to resolve the gene expression in individual cells. Data collection and imaging analysis were performed using NIH ImageJ software. Data are presented as mean ± standard error of the mean (SEM). Student's t-tests were performed to compare experimental groups ($*P < 0.05$, $**P < 0.01$, and $***P < 0.001$).

## Supporting Information

Supporting Information is available from the Wiley Online Library or from the author.

## Acknowledgements

This work was supported by the National Institutes of Health (NIH) Director's New Innovator Award (1DP2OD007161–01).

Received: June 11, 2015
Revised: July 9, 2015
Published online: August 28, 2015

[1] K. M. Yamada, E. Cukierman, *Cell* **2007**, *130*, 601.
[2] V. Lecault, A. K. White, A. Singhal, C. L. Hansen, *Curr. Opin. Chem. Biol.* **2012**, *16*, 381.
[3] D. Tautz, C. Pfeifle, *Chromosoma* **1989**, *98*, 81.
[4] F. Wang, J. Flanagan, N. Su, L. C. Wang, S. Bui, A. Nielson, X. Wu, H. T. Vo, X. J. Ma, Y. Luo, *J. Mol. Diagn.* **2012**, *14*, 22.
[5] R. Sandberg, *Nat. Methods* **2014**, *11*, 22.
[6] M. De, P. S. Ghosh, V. M. Rotello, *Adv. Mater.* **2008**, *20*, 4225.
[7] L. Vigderman, B. P. Khanal, E. R. Zubarev, *Adv. Mater.* **2012**, *24*, 4811.
[8] R. Riahi, M. Long, Y. Yang, Z. Dean, D. D. Zhang, M. J. Slepian, P. K. Wong, *Integr. Biol.* **2014**, *6*, 192.
[9] Y. Kam, A. Rubinstein, S. Naik, I. Djavsarov, D. Halle, I. Ariel, A. O. Gure, A. Stojadinovic, H. Pan, V. Tsivin, A. Nissan, E. Yavin, *Cancer Lett.* **2014**, *352*, 90.
[10] S. Tyagi, *Nat. Methods* **2009**, *6*, 331.
[11] D. S. Seferos, D. A. Giljohann, H. D. Hill, A. E. Prigodich, C. A. Mirkin, *J. Am. Chem. Soc.* **2007**, *129*, 15477.
[12] D. Zheng, D. S. Seferos, D. A. Giljohann, P. C. Patel, C. A. Mirkin, *Nano Lett.* **2009**, *9*, 3258.
[13] T. L. Halo, K. M. McMahon, N. L. Angeloni, Y. L. Xu, W. Wang, A. B. Chinen, D. Malin, E. Strekalova, V. L. Cryns, C. H. Cheng, C. A. Mirkin, C. S. Thaxton, *Proc. Natl. Acad. Sci. USA* **2014**, *111*, 17104.
[14] Z. S. Dean, R. Riahi, P. K. Wong, *Biomaterials* **2015**, *37*, 156.
[15] R. Riahi, S. Wang, M. Long, N. Li, P. Y. Chiou, D. D. Zhang, P. K. Wong, *ACS Nano* **2014**, *8*, 3597.
[16] J. P. Giraldo-Vela, W. Kang, R. L. McNaughton, X. Zhang, B. M. Wile, A. Tsourkas, G. Bao, H. D. Espinosa, *Small* **2015**, *11*, 2386.
[17] B. Xiong, K. Ren, Y. Shu, Y. Chen, B. Shen, H. Wu, *Adv. Mater.* **2014**, *26*, 5525.
[18] D. A. Jaitin, E. Kenigsberg, H. Keren-Shaul, N. Elefant, F. Paul, I. Zaretsky, A. Mildner, N. Cohen, S. Jung, A. Tanay, I. Amit, *Science* **2014**, *343*, 776.
[19] R. Riahi, Z. Dean, T. H. Wu, M. A. Teitell, P. Y. Chiou, D. D. Zhang, P. K. Wong, *Analyst* **2013**, *138*, 4777.
[20] B. Vester, J. Wengel, *Biochemistry* **2004**, *43*, 13233.
[21] M. Petersen, J. Wengel, *Trends Biotechnol.* **2003**, *21*, 74.
[22] G. P. Acuna, M. Bucher, I. H. Stein, C. Steinhauer, A. Kuzyk, P. Holzmeister, R. Schreiber, A. Moroz, F. D. Stefani, T. Liedl, F. C. Simmel, P. Tinnefeld, *ACS Nano* **2012**, *6*, 3189.
[23] T. G. Iversen, T. Skotland, K. Sandvig, *Nano Today* **2011**, *6*, 176.
[24] S. Arima, K. Nishiyama, T. Ko, Y. Arima, Y. Hakozaki, K. Sugihara, H. Koseki, Y. Uchijima, Y. Kurihara, H. Kurihara, *Development* **2011**, *138*, 4763.
[25] R. Benedito, C. Roca, I. Sorensen, S. Adams, A. Gossler, M. Fruttiger, R. H. Adams, *Cell* **2009**, *137*, 1124.
[26] M. Hellstrom, L. K. Phng, J. J. Hofmann, E. Wallgard, L. Coultas, P. Lindblom, J. Alva, A. K. Nilsson, L. Karlsson, N. Gaiano, K. Yoon, J. Rossant, M. L. Iruela-Arispe, M. Kalen, H. Gerhardt, C. Betsholtz, *Nature* **2007**, *445*, 776.
[27] J. Sun, N. Jamilpour, F. Y. Wang, P. K. Wong, *Biomaterials* **2014**, *35*, 3273.
[28] S. Artavanis-Tsakonas, M. D. Rand, R. J. Lake, *Science* **1999**, *284*, 770.
[29] M. E. Fortini, *Dev. Cell* **2009**, *16*, 633.
[30] R. Riahi, J. Sun, S. Wang, M. Long, D. D. Zhang, P. K. Wong, *Nat. Commun.* **2015**, *6*, 6556.
[31] R. Riahi, Y. L. Yang, D. D. Zhang, P. K. Wong, *J. Lab. Autom.* **2012**, *17*, 59.
[32] J. Sun, Y. Xiao, S. Wang, M. J. Slepian, P. K. Wong, *J. Lab. Autom.* **2015**, *20*, 127.